

An isolated Dirac cone on the surface of ternary tetradymite-like topological insulators

This article has been downloaded from IOPscience. Please scroll down to see the full text article.

2011 New J. Phys. 13 095005

(<http://iopscience.iop.org/1367-2630/13/9/095005>)

View [the table of contents for this issue](#), or go to the [journal homepage](#) for more

Download details:

IP Address: 204.121.6.216

The article was downloaded on 07/02/2012 at 05:01

Please note that [terms and conditions apply](#).

An isolated Dirac cone on the surface of ternary tetradymite-like topological insulators

H Lin^{1,4}, Tanmoy Das^{1,2}, L A Wray³, S-Y Xu³, M Z Hasan³
and A Bansil¹

¹ Department of Physics, Northeastern University, Boston, MA 02115, USA

² Theoretical Division, Los Alamos National Laboratory, Los Alamos, NM 87545, USA

³ Joseph Henry Laboratories of Physics, Princeton University, Princeton, NJ 08544, USA

E-mail: nilnish@gmail.com

New Journal of Physics **13** (2011) 095005 (6pp)

Received 27 May 2011

Published 9 September 2011

Online at <http://www.njp.org/>

doi:10.1088/1367-2630/13/9/095005

Abstract. We have extended the search for topological insulators to the ternary tetradymite-like compounds M_2X_2Y ($M = \text{Bi}$ or Sb ; X and $Y = \text{S}$, Se or Te), which are variations of the well-known binary compounds Bi_2Se_3 and Bi_2Te_3 . Our first-principles computations suggest that five existing compounds are strong topological insulators with a single Dirac cone on the surface. In particular, stoichiometric $\text{Bi}_2\text{Se}_2\text{S}$, $\text{Sb}_2\text{Te}_2\text{Se}$ and $\text{Sb}_2\text{Te}_2\text{S}$ are predicted to have an isolated Dirac cone on their naturally cleaved surface. This finding paves the way for the realization of the topological transport regime.

A topological insulator is a very distinct state of quantum matter with a bulk-insulating gap of spin-orbit coupling (SOC) origin (for a brief review, see [1]; [2–11]). The Dirac fermions on the surface of a topological insulator possess a topological quantum Berry phase and a definite spin chirality, which protects them from back-scattering and localization, resulting in the counterpropagation of opposite spin states without dissipation. These are the key electronic ingredients for application to topological quantum computing [12, 13] and low-power spintronics [14] devices, for which, however, the dissipationless surface states must be in the topological transport regime, i.e. to have an isolated Dirac cone fully separated from the bulk bands, and the Fermi level has to lie at the Dirac point [15]. The existing topological insulating

⁴ Author to whom any correspondence should be addressed.

materials fail in this regard due to their material-specific complications, such as interference from numerous surface states [16], shielding of the Dirac cone inside either the bulk-valence band [17, 18] or the conduction bands [19], or the involvement of crystal distortion in fabricating the material [20, 21].

Recently, it was shown experimentally that an isolated Dirac cone can be achieved by tuning the Fermi level with appropriate hole doping, but the non-stoichiometric crystal structure and the requirement for surface deposition generally make this approach unsuitable for most practical applications [11, 18]. On the other hand, solid solutions in the tetradymite-like compounds provide a platform to engineer topological surface states. For example, the theoretical work of Zhang *et al* [22] indicates the presence of a topological phase transition in $\text{Sb}_2(\text{Te}_{1-x}\text{Se}_x)_3$ for $0 \leq x \leq 1$. Interestingly, since Se atoms preferentially occupy the central site in the crystal, at $x = 1/3$ the stoichiometric compound $\text{Sb}_2\text{Te}_2\text{Se}$ can admit an ordered phase. Our recent work on the topological insulator $\text{Bi}_2\text{Te}_2\text{Se}$ reveals that the linewidth of the topological surface states in angle-resolved photoemission spectroscopy is narrow, indicating that disorder effects are suppressed in these compounds [23]. Ren *et al* [24] have shown that to date $\text{Bi}_2\text{Te}_2\text{Se}$ is the most suitable material for the study of the topological surface states because it has the highest bulk resistivity among all known topological insulators.

In this paper, we report first-principles computations on five existing tetradymite-like compounds— $\text{Bi}_2\text{Te}_2\text{Se}$, $\text{Bi}_2\text{Te}_2\text{S}$, $\text{Bi}_2\text{Se}_2\text{S}$, $\text{Sb}_2\text{Te}_2\text{Se}$ and $\text{Sb}_2\text{Te}_2\text{S}$ —to show that these materials host salient topological insulating features in their stoichiometric crystal structures. Our important findings include that the last three of the five aforementioned compounds harbor an isolated Dirac cone with Dirac points that lie fully within the gap, allowing these states to reach the long-sought territory of the topological spin-transport regime [6, 15, 25], where the in-plane carrier transport would have a purely quantum topological origin.

Topological insulators in two and three dimensions have been predicted theoretically and observed experimentally to display the quantum spin Hall effect [3, 4, 26] and strong topological behavior due to the combined effects of relativistic Dirac fermions and quantum entanglement [1, 3–11]. For systems with inversion symmetry, a band inversion occurs due to a finite value of the SOC. This results in a bulk-insulating gap that ensures the existence of metallic surface states within the gap [16]. In bismuth or antimony metals, numerous surface states interfere with each other and an odd number of Dirac cones can be achieved by making composite alloys such as $\text{Bi}_{1-x}\text{Sb}_x$ [10]. In other novel classes of topological insulators, the Dirac node appears either below the valence band maximum (VBM) as in Bi_2Te_3 or Sb_2Te_3 [18] or above the conduction band minimum as in TlSbTe_2 [19]. Topologically non-trivial materials such as the half-Heusler [20] and Li_2AgSb [21] series are semi-metals, which require lattice distortion to be tuned into the topological insulating state. For these reasons, it is difficult to electrically gate these materials for the manipulation and control of charge carriers for realizing a device. Therefore, a viable route to search for the isolated Dirac node in topological insulating materials is to find a chemically stable stoichiometric composition in an appropriate class of materials.

With this motivation, we consider in this paper five existing stoichiometric tetradymite-like ternary compounds in the structure M_2X_2Y , namely $\text{Bi}_2\text{Te}_2\text{Se}$ [27], $\text{Bi}_2\text{Te}_2\text{S}$ [28], $\text{Bi}_2\text{Se}_2\text{S}$ [29], $\text{Sb}_2\text{Te}_2\text{Se}$ [30] and $\text{Sb}_2\text{Te}_2\text{S}$ [31]. The tetradymite structure is with a rhombohedral unit cell of the space group $R\bar{3}m$. The commonly invoked hexagonal cell shown in figure 1(a) consists of three quintuple layers. The stacking order of two consecutive units may be represented as $-X - M - Y - M - X - X - M - Y - M - X -$. The layer of Y atoms is in the center of the

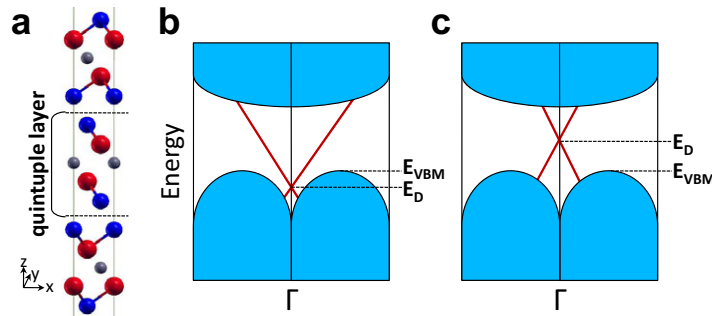


Figure 1. Tetradymite crystal structure and topological transport regime. (a) The crystal structure of the tetradymite M_2X_2Y . The M , X and Y atoms are represented by red, blue and gray balls, respectively. (b, c) Surface band structures near the Γ -point for stoichiometric Bi_2Te_3 and Bi_2Se_2S .

unit. The natural surface termination is between the two X -atom layers. The known topological insulators Bi_2Se_3 , Bi_2Te_3 and Sb_2Te_3 have the same crystal structure with $X = Y$.

Figure 1(b) shows a schematic illustration of the bulk and surface band structures of Bi_2Se_3 , Bi_2Te_3 and Sb_2Te_3 in which the surface Dirac point lies below the VBM. In our earlier experimental work, we lowered the Fermi level (E_F) of Bi_2Se_3 into the bulk bandgap by substituting trace amounts of Ca^{2+} for Bi^{3+} , with Ca acting as a hole donor to the bulk states. In order to lift the Dirac point above the VBM, we deposited NO_2 on the surface. An isolated Dirac cone is then obtained, as illustrated in figure 1(c). In this study, we predict new topological insulators Bi_2Te_2Se , Bi_2Te_2S , Bi_2Se_2S , Sb_2Te_2Se and Sb_2Te_2S , among which the latter three have a Dirac point located in the bulk gap above the VBM, as shown in figure 1(c). Therefore, these three compounds are well suited as materials with an isolated Dirac cone without requiring tuning via surface deposition. With proper electron/hole doping control or gating, one can position the E_F at the Dirac point and the material can be in the transport regime for potential device applications. We did not attempt to tune the electronic structure of the studied compounds using virtual crystal [32, 33] or other first-principles approaches [34, 35].

The first-principles band structures were computed on the basis of experimental lattice data [27–31] within the framework of the density functional theory (DFT) using the generalized gradient approximation (GGA). Our results, shown in figure 2, predict that all these materials naturally host a topological insulating phase with band gaps in the range of 224–297 meV. A band inversion occurs at the Γ -point, as highlighted by gray-shaded areas. As illustrated in figure 2(f), the conduction band (red solid line) and the valence band (blue dashed line) cross each other near the Γ -point, so that at this point the occupied state possesses the character of the conduction band and the unoccupied state possesses that of the valence band. Since the crystal has inversion symmetry, we have applied band parity analysis [5] to evaluate the value of the topological invariant Z_2 . All five compounds are thus found to be strong topological insulators with $Z_2 = -1$. This has come about due to band inversion at the Γ -point through which the Z_2 topological invariant picks up an extra factor of -1 compared to bands without SOC. In short, the presence of an energy gap throughout the Brillouin zone with a band inversion only at the Γ -point makes this class of materials topological insulators.

The calculated DFT-GGA surface bands are shown in figure 3. A pair of surface bands with opposite spin directions are degenerate at the zone center and form the Dirac-cone-like

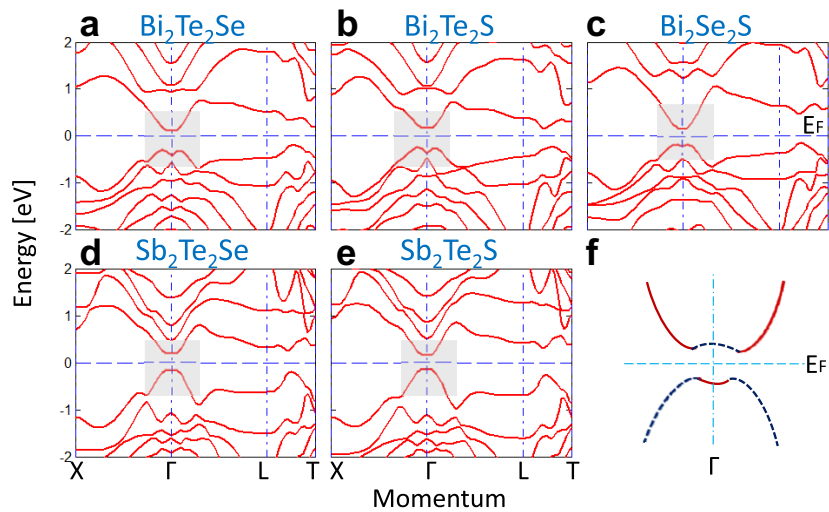


Figure 2. Bulk electronic structures and band-inversion. Bulk electronic structures of (a) $\text{Bi}_2\text{Te}_2\text{Se}$, (b) $\text{Bi}_2\text{Te}_2\text{S}$, (c) $\text{Bi}_2\text{Se}_2\text{S}$, (d) $\text{Sb}_2\text{Te}_2\text{Se}$ and (e) $\text{Sb}_2\text{Te}_2\text{S}$. The gray-shaded area in panels (a)–(e) indicate the inverted band structure illustrated in panel (f).

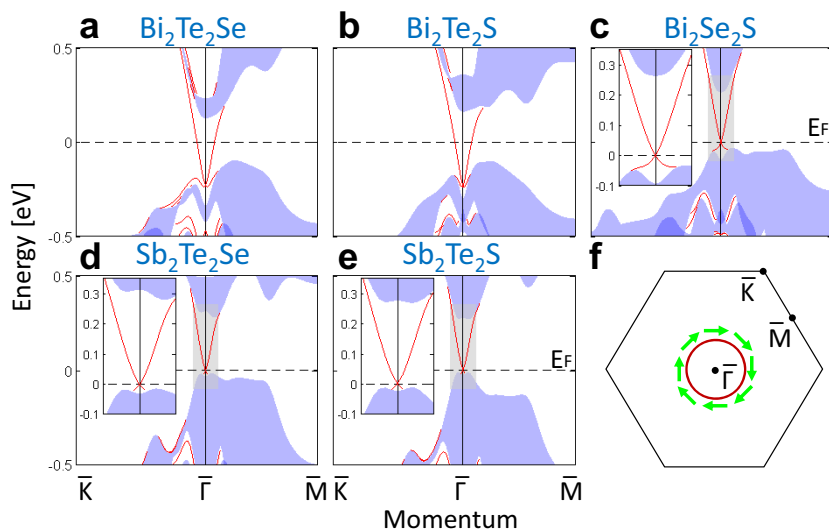


Figure 3. Surface states and spin texture of the Dirac cone. Surface band structures of (a) $\text{Bi}_2\text{Te}_2\text{Se}$, (b) $\text{Bi}_2\text{Te}_2\text{S}$, (c) $\text{Bi}_2\text{Se}_2\text{S}$, (d) $\text{Sb}_2\text{Te}_2\text{Se}$ and (e) $\text{Sb}_2\text{Te}_2\text{S}$. Red lines are the surface states and the blue shaded areas are projected bulk states. Surface momentum is defined in panel (f), showing the hexagonal surface Brillouin zone. Green arrows in panel (f) denote the spin direction of the upper Dirac cone at constant energy (blue circle).

dispersion. All five compounds exhibit a single Dirac cone inside the bulk band gap. For $\text{Bi}_2\text{Te}_2\text{Se}$ and $\text{Bi}_2\text{Te}_2\text{S}$, the Dirac point lies below the VBM. This is the same as the case of the stoichiometric binary compound Bi_2Te_3 in which bulk scattering channels at the energy of the Dirac point prevent interesting quantum phenomena in the topological transport regime

being realized. The most interesting results are found in $\text{Bi}_2\text{Se}_2\text{S}$, $\text{Sb}_2\text{Te}_2\text{Se}$ and $\text{Sb}_2\text{Te}_2\text{S}$ where an isolated Dirac cone is obtained. Here, the Dirac point lies above the VBM and below the conduction bands. When E_F is tuned to the Dirac point, the density of states approaches zero and there are no other scattering channels. Therefore, $\text{Bi}_2\text{Se}_2\text{S}$, $\text{Sb}_2\text{Te}_2\text{Se}$ and $\text{Sb}_2\text{Te}_2\text{S}$ would be stoichiometric compounds that are well suited for investigating the topological transport regime.

In conclusion, we predict that the stoichiometric tetradymite-like compounds $\text{Bi}_2\text{Te}_2\text{Se}$, $\text{Bi}_2\text{Te}_2\text{S}$, $\text{Bi}_2\text{Se}_2\text{S}$, $\text{Sb}_2\text{Te}_2\text{Se}$ and $\text{Sb}_2\text{Te}_2\text{S}$ are strong topological insulators with a large enough band gap for room temperature applications. The isolated Dirac cone on the surface of $\text{Bi}_2\text{Se}_2\text{S}$, $\text{Sb}_2\text{Te}_2\text{Se}$ and $\text{Sb}_2\text{Te}_2\text{S}$ will be particularly important for the study of topological transport properties on a bulk material without the need for surface deposition [11]. Experiments with magnetic scattering techniques should be able to uniquely access the helical spin texture of the isolated surface states that are essential for device applications. The stoichiometric crystals of the investigated compounds are very easy to produce and manipulate for the manufacture of devices for microchips [36], spintronics [14] and information [12, 13] technologies. Furthermore, the full exposure of the topological transport regime for dissipationless spin current with the unique advantage of tunable surface states is suitable for the study of novel topological phenomena such as the intrinsic quantum spin Hall effect [3, 4, 26], the universal topological magneto-electric effect [37] and anomalous half-integer quantization of Hall conductance [6, 38] and quantum electrodynamical phenomena such as the image magnetic monopole induced by an electric charge [39] or Majorana fermions induced by the proximity effects from a superconductor [12].

Methods. First-principles band calculations were performed with the linear augmented plane wave method using the WIEN2K package [40] within the framework of DFT. GGA was used to describe the exchange-correlation potential [41]. SOC was included as a second variational step using the basis of scalar relativistic eigenfunctions. The surface was simulated by placing a slab of six quintuple layers for $\text{Bi}_2\text{Te}_2\text{Se}$ and $\text{Bi}_2\text{Te}_2\text{S}$. For $\text{Bi}_2\text{Se}_2\text{S}$, $\text{Sb}_2\text{Te}_2\text{Se}$ and $\text{Sb}_2\text{Te}_2\text{S}$, we used 12 quintuple layers to ensure convergence with the number of layers.

Acknowledgments

Out work at Northeastern and Princeton was supported by the Division of Materials Science and Engineering, Basic Energy Sciences, US Department of Energy (DE-FG02-07ER46352, DE-FG-02-05ER46200 and AC03-76SF00098), and benefited from the allocation of supercomputer time at NERSC and Northeastern University's Advanced Scientific Computation Center. Support from the A P Sloan Foundation (to LAW, SYX and MZH) is also acknowledged.

References

- [1] Moore J E 2010 *Nature* **464** 194–8
- [2] Hasan M Z and Kane C L 2010 *Rev. Mod. Phys.* **82** 3045
- [3] Kane C L and Mele E J 2005 *Phys. Rev. Lett.* **95** 146802
- [4] Bernevig B A, Hughes T L and Zhang S-C 2006 *Science* **314** 1757–61
- [5] Fu L and Kane C L 2007 *Phys. Rev. B* **76** 045302
- [6] Fu L, Kane C L and Mele E J 2007 *Phys. Rev. Lett.* **98** 106803
- [7] Moore J E and Balents L 2007 *Phys. Rev. B* **75** 121306

- [8] Roy R 2009 *Phys. Rev. B* **79** 195322
- [9] König M *et al* 2007 *Science* **318** 766–70
- [10] Hsieh D *et al* 2008 *Nature* **452** 970–4
- [11] Hsieh D *et al* 2009 *Nature* **460** 1101–5
- [12] Fu L and Kane C L 2008 *Phys. Rev. Lett.* **100** 096407
- [13] Leek P J *et al* 2007 *Science* **318** 1889–92
- [14] Wolf S A *et al* 2001 *Science* **294** 1488–95
- [15] Fu L and Kane C L 2009 *Phys. Rev. Lett.* **102** 216403
- [16] Zhang H *et al* 2009 *Nat. Phys.* **5** 438–42
- [17] Xia Y *et al* 2009 *Nat. Phys.* **5** 398–402
- [18] Hsieh D *et al* 2009 *Phys. Rev. Lett.* **103** 146401
- [19] Lin H *et al* 2010 *Phys. Rev. Lett.* **105** 036404
- [20] Lin H *et al* 2010 *Nat. Mater.* **9** 546
- [21] Lin H *et al* 2010 arXiv:1004.0999
- [22] Zhang W *et al* 2010 *New J. Phys.* **12** 065013
- [23] Xu S-Y *et al* 2010 arXiv:1007.5111v1
- [24] Ren Z *et al* 2010 *Phys. Rev. B* **82** 241306
- [25] Qi X-L, Hughes T L and Zhang S-C 2008 *Phys. Rev. B* **78** 195424
- [26] Bernevig B A and Zhang S-C 2006 *Phys. Rev. Lett.* **98** 106802
- [27] Mishra S and Bever M B 1964 *J. Phys. Chem. Solids* **25** 1233–41
- [28] Harker D 1934 *Z. Kristallogr.* **89** 175–81
- [29] Chichagov A V *et al* 1990 (MINCRYST) *Kristallographya* **35** 610–16
- [30] Anderson T L and Krause H B 1974 *Acta Crystallogr. B* **30** 1307
- [31] Grauer D C, Hor Y S, Williams A J and Cava R J 2009 *Mater. Res. Bull.* **44** 1926–9
- [32] Bansil A 1993 *Z. Nat.forsch. A* **48** 165
- [33] Lin H, Sahrakorpi S, Markiewicz R S and Bansil A 2006 *Phys. Rev. Lett.* **96** 097001
- [34] Bansil A, Kaprzyk S, Mijnaerends P E and Tobola J 1999 *Phys. Rev. B* **60** 13396
Mijnaerends P E and Bansil A 1976 *Phys. Rev. B* **13** 2381–90
- [35] Khanna S N, Ibrahim A K, McKnight S W and Bansil A 1985 *Solid State Commun.* **55** 223–6
Huisman L, Nicholson D, Schwartz L and Bansil A 1981 *Phys. Rev. B* **24** 1824–34
- [36] Seradjeh B, Moore J E and Franz M 2009 *Phys. Rev. Lett.* **103** 066402
- [37] Essin A, Moore J E and Vanderbilt D 2009 *Phys. Rev. Lett.* **102** 146805
- [38] Qi X-L, Hughes T L and Zhang S-C 2008 *Phys. Rev. B* **78** 195424
- [39] Qi X-L, Li R, Zhang J and Zhang S-C 2009 *Science* **323** 1184
- [40] Blaha P, Schwarz K, Madsen G K H, Kvasnicka D and Luitz J 2001 *WIEN2k, an Augmented Plane Wave Plus Local Orbitals Program for Calculating Crystal Properties* (Vienna, Austria: Karlheinz Schwarz, Technical University Wien)
- [41] Perdew J P, Burke K and Ernzerhof M 1996 *Phys. Rev. Lett.* **77** 3865–8